

THE OFFICIAL MAGAZINE OF THE OCEANOGRAPHY SOCIETY

Oceanography

CITATION

Ager, T.P. 2013. An introduction to synthetic aperture radar imaging. *Oceanography* 26(2):20–33, <http://dx.doi.org/10.5670/oceanog.2013.28>.

DOI

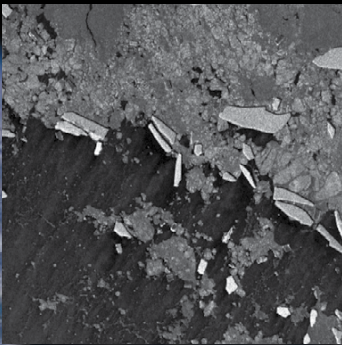
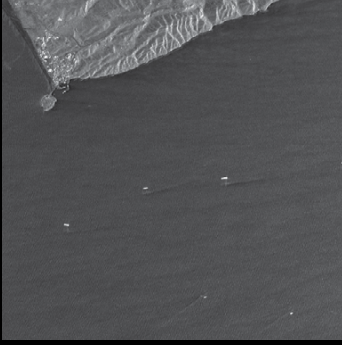
<http://dx.doi.org/10.5670/oceanog.2013.28>

COPYRIGHT

This article has been published in *Oceanography*, Volume 26, Number 2, a quarterly journal of The Oceanography Society. Copyright 2013 by The Oceanography Society. All rights reserved.

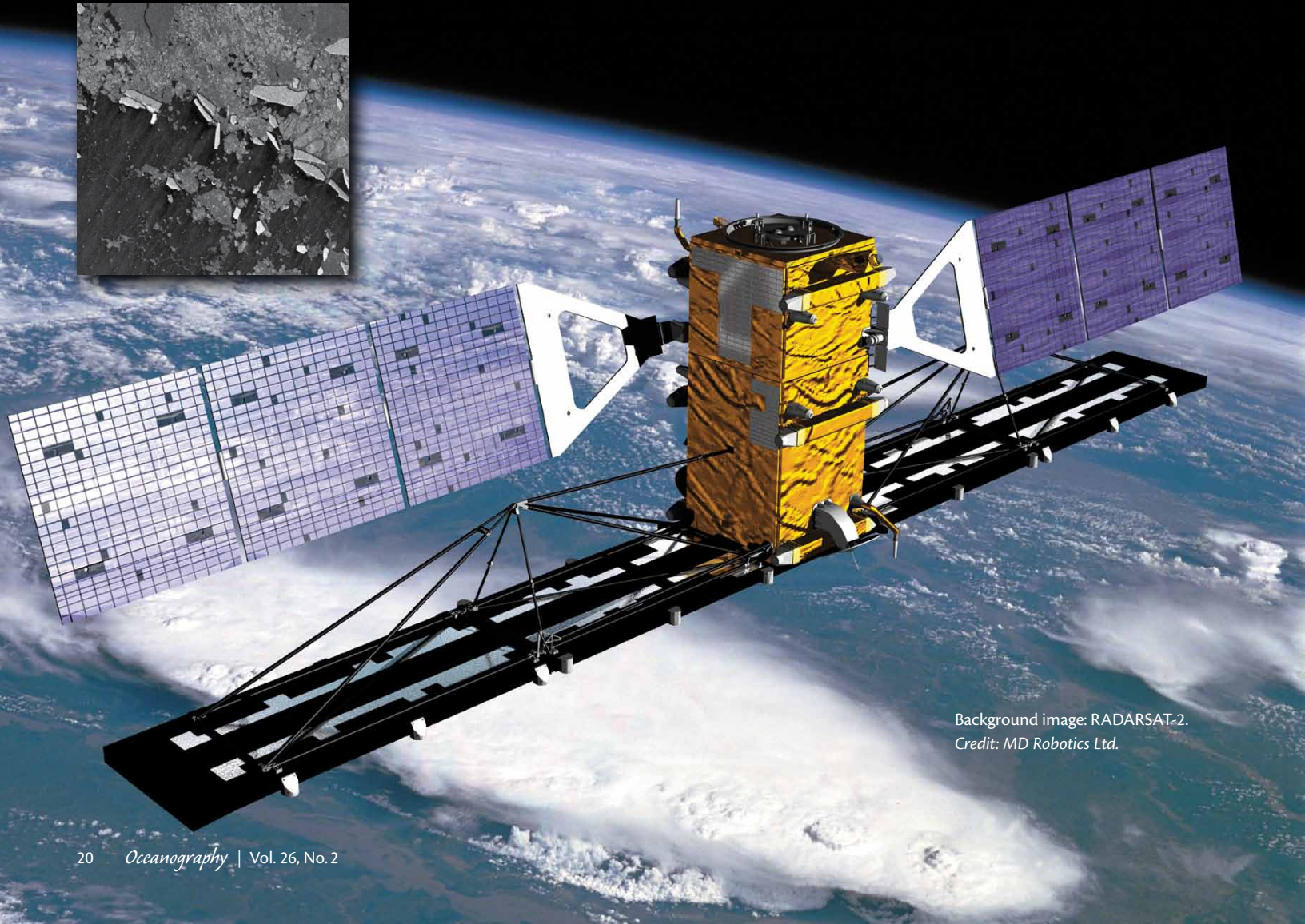
USAGE

Permission is granted to copy this article for use in teaching and research. Republication, systematic reproduction, or collective redistribution of any portion of this article by photocopy machine, reposting, or other means is permitted only with the approval of The Oceanography Society. Send all correspondence to: info@tos.org or The Oceanography Society, PO Box 1931, Rockville, MD 20849-1931, USA.



An Introduction to Synthetic Aperture Radar Imaging

BY THOMAS P. AGER



Background image: RADARSAT-2.
Credit: MD Robotics Ltd.

THE VALUE OF RADAR IMAGING

RADAR is an acronym for Radio Detection and Ranging. Its ability to determine range and motion make it suitable for many applications, such as air traffic control, vehicle speed detection on roadways, and storm tracking. Radar is also used as an active imaging technology in which pulses of microwave energy are emitted from an antenna and the resulting reflections are used to create images.

Radar's most important attribute for imaging applications is that its relatively long wavelengths penetrate clouds, dust, and even volcanic ash, and it can image independent of most weather conditions. Considering that this is an ocean planet, with vast amounts of water vapor continuously condensing into clouds over large regions of Earth's surface, radar is a core remote-sensing technology and it becomes the primary imaging source when cloud cover prevents other means of data collection.

Table 1 shows the distribution of frequencies (f) and wavelengths (λ) of the established radar bands. The wavelengths are very much longer than those of visible light. Radar imaging systems avoid wavelengths shorter than K-band because these

are reflected by water vapor and other atmospheric particles. In fact, high-frequency microwave bands are used in Doppler radar weather instruments to detect rain and storms. The more typical imaging bands are X-band, C-band, and some of the very long wavelength bands. The wavelengths of L-band and ultra-high-frequency (UHF) radar are so long that they can penetrate foliage and are sometimes used to image through tree canopy in forested areas.

Aside from cloud-cover penetration, radar has other notable characteristics that make it valuable for remote-sensing applications:

- Because radar provides its own illumination, data can be collected independent of sunlight during the day or at night.
- The technique called synthetic aperture radar (SAR) provides high resolution with the remarkable characteristic that its resolution does not degrade with distance. Distance weakens the strength of the radar reflections and can increase image noise, but as will be shown later in this paper, resolution cell size does not increase as distance increases.
- Because radars do not have a fixed lens, as do optical systems, they are flexible regarding resolution and ground coverage, so that a single system can collect data from wide areas at low resolution, medium areas at medium resolution, and small areas at high resolution.
- The measurements radar makes are naturally precise, and radar imaging systems can be configured to have outstanding geometric accuracy (Ager, 2001).
- Finally, and perhaps most importantly, radar illumination is coherent. Radar antennas emit pulses of microwave energy in which the characteristics of the waves are controlled and consistent pulse to pulse. This natural coherence enables the creation of products such as digital elevation models and sensitive measurements of Earth surface changes over time.

Table 1. Designations for radar frequency bands (IEE Standard 521-1984).

Band	Frequency Range (GHz)		Wavelength Range (cm)	
UHF	0.3	1	100	30
L	1	2	30	15
S	2	4	15	7.5
C	4	8	7.5	3.75
X	8	12	3.75	2.5
Ku	12	18	2.5	1.67
K	18	27	1.67	1.11
Ka	27	40	1.11	0.75
V	40	75	0.75	0.40
W	75	110	0.40	0.27
mm	110	300	0.27	0.10

Thomas P. Ager (tomagerllc@gmail.com) is President, Tomager LLC, Geomatics Consulting and Training, Lansdowne, VA.

RADAR AS AN ECHO MEASUREMENT SYSTEM

A radar antenna emits individual pulses of microwave radiation. The pulses are sent at a pulse repetition frequency (PRF) in the range of 2,000 per second or more. As Figure 1 shows, these pulses are scattered in every direction, and a small portion, called radar backscatter, is returned to the antenna. The radar measures the characteristics of the echoes, including the round-trip time for the pulse to travel from the antenna to the ground and back to the antenna, the strength of the reflection, and the phase of the return wave. That is, the radar can determine if the wave returns at its peak, trough, or somewhere in between.

The pulse travel time is used to determine the range from the antenna to the ground. Range is simple to calculate and is merely equal to the pulse speed, which is the known speed of light, multiplied by the round-trip time divided by two:

$$\text{Range} = \frac{c\Delta T}{2}.$$

Radar data associated with these pulse measurements are often referred to as the “fast-time” dimension, while the motion of the sensor along its flight path is called “slow-time.”

Figure 2 shows the measurement of the strength of the backscatter as a function of time. In this example, the pulse reflects first in the near-range area. Most of the associated reflection

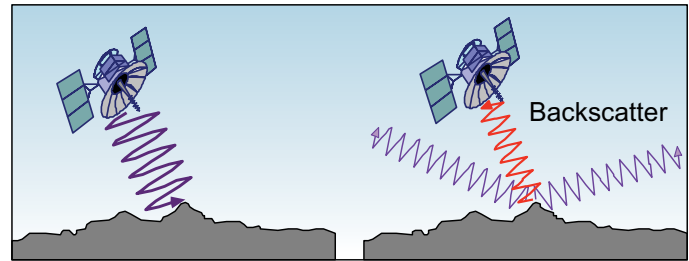


Figure 1. Radar backscatter.

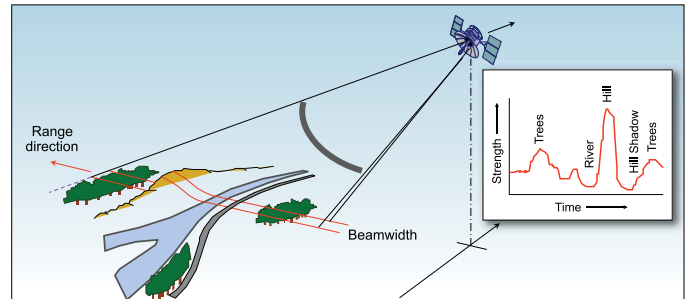


Figure 2. Measuring the backscatter.

from the flat terrain travels away from the antenna, and thus the measured backscatter is relatively weak. This is followed by a stronger backscatter, caused by the texture of the trees, and then a very weak return from the calm river. The reflection of the front side of the hill is very strong, which would result in bright pixels on the radar image.

RADAR COLLECTION GEOMETRY

Airborne and spaceborne radar sensors image off to the side of the sensor’s flight path. Most radars collect data at an angle that is orthogonal to the flight direction; Figure 3 shows this as the broadside direction. Some radars can squint the collection to image the area in front of or behind the broadside angle.

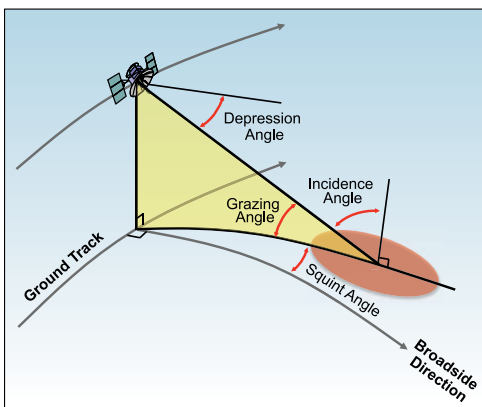


Figure 3. Radar collection angles.

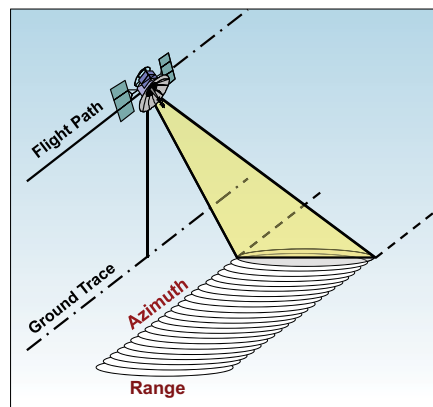


Figure 4. Radar range and azimuth dimension.

The angle down from the horizon is called the depression angle. The incidence angle is formed between the vector that is perpendicular to level at a particular location and the line between that point and the antenna. The grazing angle is the complement to the incidence angle. That is, an incidence angle of 55° is equivalent to a graze angle of 35° and vice versa.

Figure 4 shows a simple collection in which a radar is imaging broadside and compiling a long image swath by combining many thousands of individual pulses. This creates radar images with range and azimuth dimensions. Range refers to the dimension along the broadside angle, and azimuth is orthogonal to that direction.

AN OVERVIEW OF RADAR IMAGE CHARACTERISTICS

Reflectance Variations

The look of radar images is determined by the collection geometry, the manner in which energy strikes and reflects from an object, and the reflectance characteristics of the object. In the examples provided in Figure 5, the trees create a diffuse reflection, which would normally result in moderate backscatter and gray pixels on the image. Keep in mind, however, that very long radar wavelengths like UHF-band would not reflect from the trees at all, but would instead travel through the leaves and reflect from tree trunks and the ground surface. Objects hidden beneath forest canopy would be apparent in such images. Water is normally flat with respect to the long microwaves and strongly reflects energy away from the antenna; thus, it often is very dark on radar images. However, if the water surface is rougher, as it often is in the open ocean, the reflections from waves will be relatively bright compared to the background. Vertical objects like buildings produce strong returns and appear white on radar images.

The combined effects of these diffuse, specular, and corner reflections (see Figure 5) are apparent in the airborne image of Washington, DC, shown in Figure 6. Perhaps the most notable aspect of the image is the clear distinction between the Potomac and Anacostia Rivers and the land surface. Many corner reflections can be seen in the bridges and in the buildings of downtown DC.

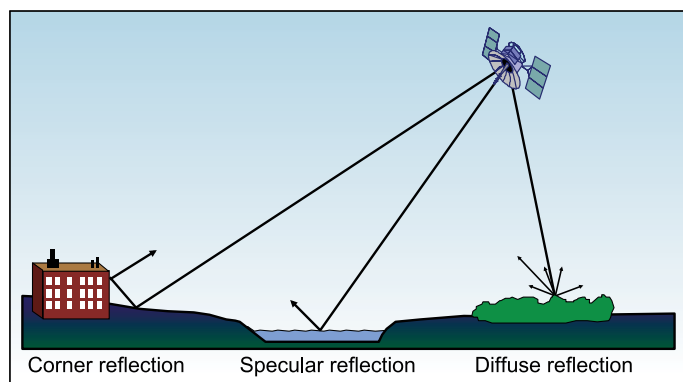


Figure 5. Reflectance variations.



Figure 6. Radar image of Washington, DC, Ku-band airborne sensor. Image courtesy of Sandia National Labs

Radar Shadows

In the radar collection shown in Figure 7, the microwave energy illuminates the mountain and the areas in front of and behind it. As noted earlier, the front face of the mountain, which has a smaller local incidence angle, reflects strongly and creates bright pixels, while the surrounding areas produce varying shades of gray. The far side of the mountain is not illuminated at all because the mountain blocks the radar energy in that area. In contrast to the dark shadows on optical images, radar shadows are black. They are actually null areas because there is no reflection, but they may include signal noise and other image artifacts.

Radar shadows cannot be manipulated by adjusting the contrast or brightness of an image as can be done for optical images. If the sun illuminated this mountain from a similar angle, its direct rays would be blocked in exactly the same way, but sunlight is attenuated by the atmosphere and is scattered sufficiently to illuminate the blocked regions. In the image of the US Capitol (Figure 8), the energy is arriving from the top of the scene and shadows fall off the back side of the buildings.

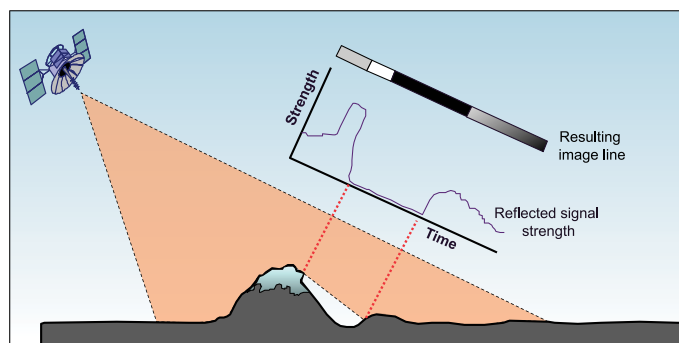


Figure 7. Geometry of radar shadow.



Figure 8. Radar shadows of US Capitol, Washington, DC. Image Courtesy Sandia National Labs

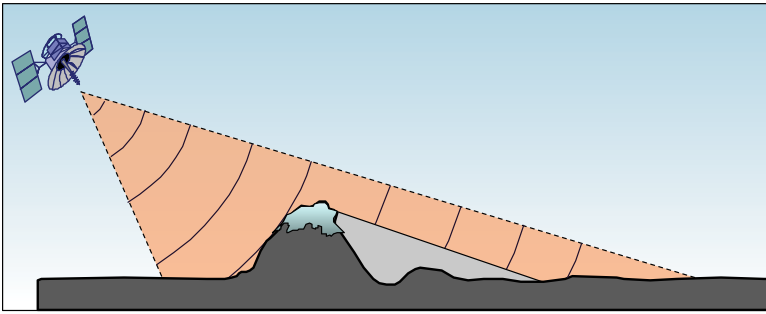


Figure 9. Radar foreshortening.

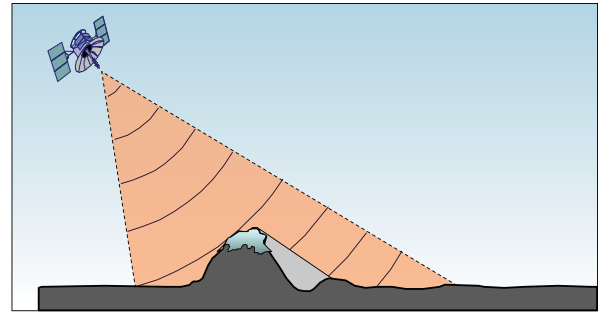


Figure 11. Radar layover.

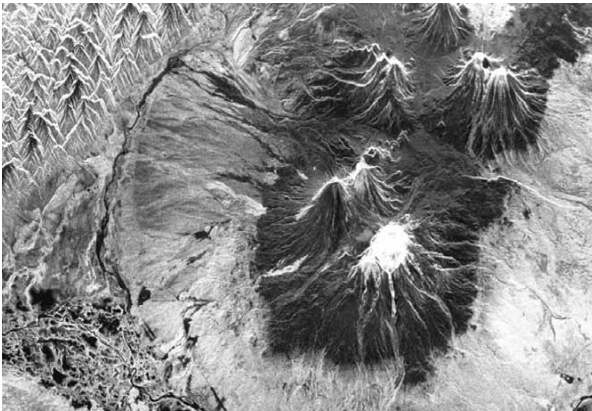


Figure 10. Radar foreshortening in SIR-C image, Kamchatka, Russia. Courtesy of NASA

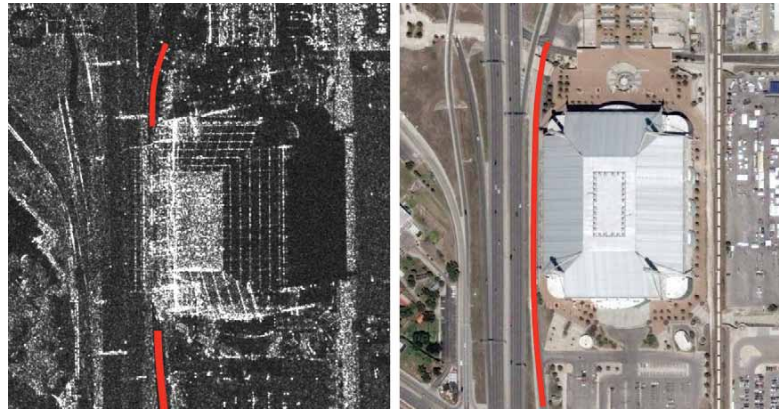


Figure 12. Radar layover of Alamo Dome, San Antonio, Texas. (left) © Astrium Services / Infoterra GmbH; (right) ©Digital Globe

Foreshortening and Layover

Another interesting characteristic of radar imaging is the manner in which elevated objects are projected onto a radar image. Radar determines the pixel location of a reflecting object in part based on its range. Notice that the sloped front end of the mountain in Figure 9 has a very small variation in range. This means that the entire front face of the mountain will be compressed on the image into the space of only a few pixels; this is called foreshortening. This effect can be seen in image from the NASA SIR-C radar mission shown in Figure 10. In that image, the energy arrives from the top and strikes the facing slopes with very little range variation, resulting in compressed, bright signatures.

Figure 11 shows a mountain illuminated from a steeper angle. In this case, the top of the mountain has the same range as the area to the left of the mountain. This means that the mountain peak and the flat area with the identical range would occupy the same pixel on the image. The mountain would lean to that area with an effect called layover. Layover is common for mountains and always occurs for towers and buildings. The degree of layover increases with steeper collection angles, and

the direction of layover is perpendicular to the flight direction of the sensor.

The radar image shown at left in Figure 12 is from the TerraSAR-X space radar system. The radar illumination came from the left in this image and the sensor motion was up toward the top of the image. Layover is perpendicular to the sensor motion, and the building leans to the left. Notice that the signature of the access road is partially blocked by the displaced signature of the roof of the Alamo dome. This image also includes a foreshortened view of the left side of the Alamo dome roof and the black shadow of the building on the right.

Foreshortening and layover are often discussed as unique radar image characteristics, but optical images display similar effects on oblique imagery. Tall objects lean over on optical images due to relief displacement, and pixels on the far side of oblique images are compressed in scale. These distortions tend to be more prominent on radar images because they must always be taken from an angle; they cannot be imaged at nadir like the Digital Globe optical image shown at right in Figure 12 (see Oliver and Quegan, 2004, for details on SAR imagery characteristics).

A FEW NOTES ON POLARIZATION

Radar and other forms of electromagnetic radiation consist of electric and magnetic fields that are perpendicular to each other. The polarization of an electromagnetic wave refers to the orientation of the electric field. If the electric field is oriented vertically with respect to Earth's surface, as shown on the left in Figure 13, then the wave is said to be vertically polarized. Because radars emit coherent radiation, the polarization is controlled and the sensor can be configured to emit and record waves of a chosen polarization. The look of the final image will be different depending on the polarization used to illuminate the ground and the physical structure of the reflecting objects. For example, tall objects scatter vertical polarized energy more prominently than horizontal polarized energy, while power lines reflect more strongly from horizontal polarization.

While polarization of an electromagnetic wave can take a range of orientations, imaging radars typically use vertical or horizontal pulses or some combination of the two (see Van Zyl and Yunjin, 2011, for a comprehensive discussion). For example, a radar might transmit horizontal pulses and record the horizontally oriented portion of the backscatter. Such a system is called HH, denoting a horizontal transmit and a horizontal receive. However, when a pulse of a particular polarization strikes an object, a portion of the backscatter energy may be flipped in orientation. Thus, it is possible to arrange for the

transmit and receive cycles to handle different polarizations. The transmit might be H, but the receive could be tuned to V, which is denoted HV and is called cross-polarization.

The image of San Francisco on the left in Figure 14 has an HH polarization. In this case, RADARSAT-2 emitted horizontally polarized waves and it recorded the horizontally polarized backscatter. The middle image has an HV polarization. Notice that the signatures of the two scenes are quite different. Cross-polarization is often useful in ship detection applications because, under some conditions, it suppresses the signature of the open ocean while providing bright signatures for ships. On the other hand, HH polarization retains the ocean signature and can sometimes be used to record wake signatures. The different signatures of the ocean surface are quite evident in these two images. Such dual-polarized collections (HH, HV) can be used together for improved ship-detection capabilities.

Some radars have the ability to change the polarization from one pulse to the next. The RADARSAT-2 images in Figure 14 were all collected during a single image operation, called quad-pol collection, in which the antenna alternately emitted H and V waves and recorded HH, HV, VV, and VH data (MacDonald, Dettwiler and Associates Ltd., 2009). The HV and VH images are alike, and a quad-pol collection actually produces three distinct images. Figure 15 shows these images combined into

a false-color composite produced by projecting the HH image in red, the HV in green, and the VV in blue. In this way, many ground cover features can be distinguished.

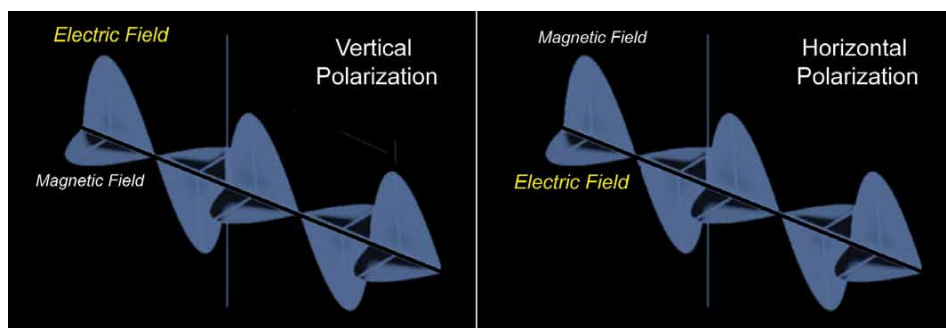


Figure 13. Vertical and horizontal polarization.

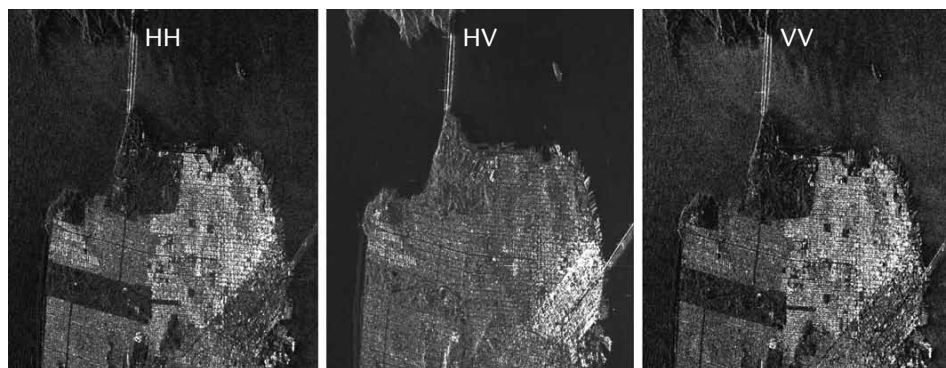


Figure 14. Multipolarized radar images. © MacDonald, Dettwiler and Associates Ltd. All Rights Reserved



Figure 15. Multipolarized false-color composite. © MacDonald, Dettwiler and Associates Ltd. All Rights Reserved

APERTURE SYNTHESIS: THE REMARKABLE STORY OF SAR IMAGE RESOLUTION

SAR Azimuth Resolution

To appreciate the power of synthetic aperture radar imaging, it is useful to first consider the resolution limitations of real aperture radars. In the early days of radar imaging, it was not possible to create images of good resolution from long standoff distances. This is because the resolution in the azimuth dimension was equivalent to the size of the beam pattern on the ground. Figure 16 illustrates that azimuth resolution for a real aperture radar is dependent on the beamwidth (β), which widens from near to far range. The size of the ground resolution cell for such a system is the beamwidth times the range. For this reason, early imaging radars had azimuth resolutions in the hundreds of meters.

Because the beamwidth is a function of the width (d) in the azimuth dimension of a rectangular antenna ($\beta = \lambda/d$), larger antennas could improve resolution. However, it was just not possible to build antennas large enough to provide good azimuth resolution. The SAR technique was developed in the early 1950s to overcome this problem, but it was not until the mid-1980s that it came into widespread use.

SAR uses the different locations of the sensor, as it moves along the flight path recording the backscatter echoes, to simulate, or synthesize, a large antenna from a small one. In the imaging process, the individual transmit and receive cycles are completed from many locations as the sensor moves. In the SAR process, these locations are treated as if they were the array elements of a single long antenna strung out along the flight path. All of the measurements of time, amplitude, and phase, which are collected sequentially, are treated as if they were collected simultaneously from one very long antenna.

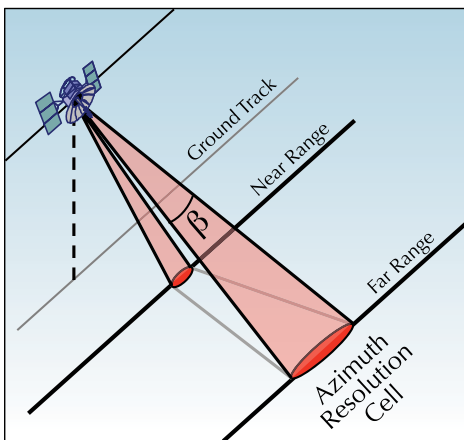


Figure 16. Azimuth resolution for real aperture radar.

Figure 17 shows a radar antenna illuminating the Strait of Gibraltar with thousands of pulses to form one large synthetic aperture. This collection ensures that the reflections are recorded from each of the many receive locations, forming a huge aperture. These locations cannot be separated by more than one-half the antenna length, which determines the minimal rate at which the pulses must be emitted, called the pulse repetition frequency. In the case of commercial space radars like COSMO-SkyMed, TerraSAR-X, and RADARSAT-2, the illumination may last two or three seconds, creating a synthetic aperture up to 20 km long (see German Aerospace Center, 2010; Italian Space Agency, 2009; MacDonald, Dettwiler and Associates Ltd., 2009).

Aperture synthesis is based on the coherent nature of radar illumination. The antenna measures the phase of each of the returns with exquisite precision. For any particular ground reflector, the phase of its echo changes at each receive location. The radar records the “phase history” of the echoes, and SAR image formation is referred to as phase history processing. SAR azimuth resolution turns out to be dependent only on the wavelength of the microwave energy and the angle subtended by the synthetic aperture:

$$\text{SAR azimuth resolution} = \frac{\lambda}{2\Delta\theta}.$$

This has the remarkable characteristic of being independent of distance. For a given radar band, SAR azimuth resolution does not degrade when the coherent collection angle is maintained. Notice in Figure 18 that the aperture length naturally increases for longer ranges when $\Delta\theta$ remains constant. SAR azimuth resolution can be quite small, even for spaceborne radars.

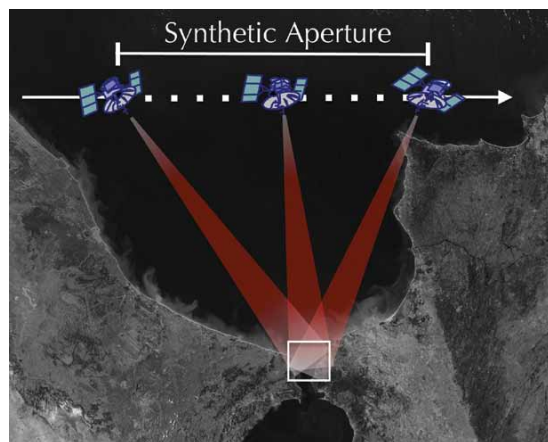


Figure 17. Aperture synthesis. Image Courtesy of NASA

The commercial space radars currently available are all capable of 1 m azimuth resolution even over ranges that approach 1,000 km. (Aperture synthesis and SAR processing are covered in many classic texts, including Ulaby et al., 1986a,b,c; Curlander and McDonough, 1991; Carrara et al., 1995; Jakowatz et al., 1996; Stimson, 1998.)

Spotlight and Stripmap Modes

The collection scheme shown in Figure 18 is called spotlight mode. For spotlight collections, the radar beam is steered to a fixed region on the ground, similar to a spotlight beam, producing images with high resolution and limited ground coverage. In contrast, stripmap collection (see Figure 19) is similar to a push-broom collection for optical images, and it collects long image swaths at medium resolution. Stripmap collection combines data from pulses with overlapping, wide angular footprints.

Stripmap collections have shorter synthetic apertures than spotlight images. These are equivalent to the beam footprint on the ground, but the image collection area is much larger. Unlike the case of brute force radar, where the beam footprint was equivalent to the azimuth resolution cell, here, the beam footprint establishes the size of the synthetic aperture. In direct contrast to real aperture radars, wider SAR beams provide better resolution.

Stripmap azimuth resolution is the length of the physical antenna (d) divided by 2:

$$\text{Stripmap azimuth resolution} \geq \frac{d}{2}.$$

This equation can be derived from the more general expression for SAR azimuth resolution. The beamwidth angle (λ/d) for stripmap SAR is equivalent to the coherent collection angle ($\Delta\theta$), and substituting beamwidth into the general equation yields the stripmap equation.

It may seem that using a very small antenna would yield excellent stripmap azimuth resolution. While this is technically true, use of a small antenna also reduces power, produces more noise in the radar image, and requires very high pulse repetition

frequencies. It is possible to use a 5 m antenna in space to yield ~ 3 m stripmap azimuth resolution, but anything much smaller than this is not feasible. Spotlight mode can produce high-resolution images via large, powerful antennas with low noise.

A Note Regarding the Doppler Shift

The Doppler shift is the apparent shift in frequency caused by the relative motion between the source of a wave and the listening device. The classic example of this phenomenon is a train whistle, in which a constant pitch seems to be shifted up while the train is approaching a stationary listener, and shifted down after the train passes. There is a widespread misunderstanding that Doppler shift is the basis of SAR processing. The term “Doppler” is used frequently in SAR terminology, as in “Doppler Phase History” and “Doppler Cone Angle,” for example. Also, many online SAR tutorials explain SAR processing as a function of Doppler shifts. This is not correct.

All of the radar echoes are indeed affected by the Doppler shift, but Doppler frequency variations are not needed for aperture synthesis. SAR processing is based on the phase variations caused by the different receive locations of the antenna. These phase variations are greater for longer synthetic apertures because the echoes are recorded in more locations. The Doppler shift has nothing to do with it. Consider that the phase variations do not require motion; they could be recorded via a series of fixed antennas that happen to replicate the sensor receive locations. In this case, there would be no Doppler shift, yet an identical image would be formed. Doppler shifts do occur in radar imaging, but they are removed in processing, and they are not needed to synthesize the large antenna.

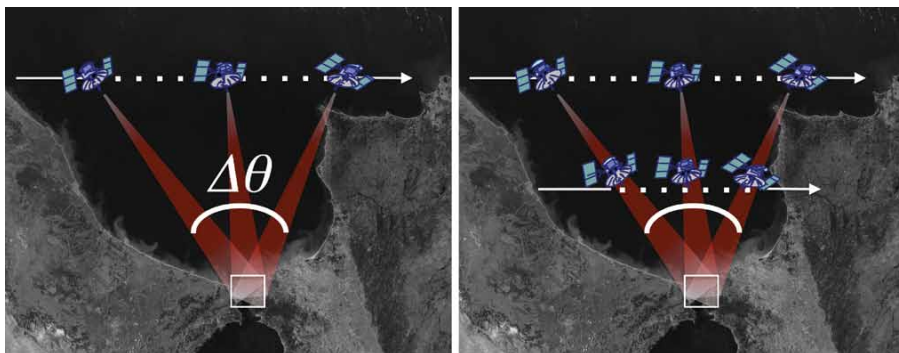


Figure 18. Coherent collection angle in spotlight mode. Image Courtesy of NASA

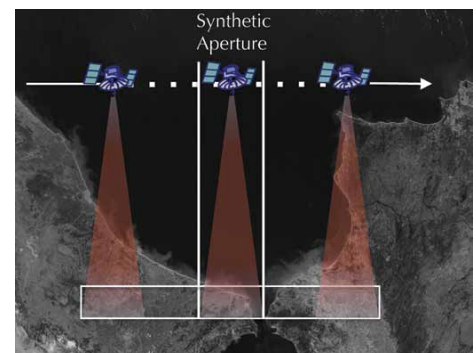


Figure 19. Synthetic aperture for stripmap SAR. Image Courtesy of NASA

Improving Range Resolution

As in the discussion of azimuth resolution, we will first consider range resolution for a simple radar, observe that it cannot provide good resolution, and then fix the problem to produce a resolution equation that is again independent of distance.

Consider the illustration in Figure 20. It shows a radar pulse emitted from an antenna and reflecting from two houses. The pulse is emitted at light speed for some very short duration, so it has a pulse length equal to c times that pulse duration. This long pulse strikes the first house and reflects from it. It then continues to the second house, and the front end of the pulse begins to reflect, while the back end of the pulse continues toward the house. In this case, the two houses are sufficiently separate in space to generate two distinct reflections. The situation is a bit different in Figure 21. In this case, the two houses are closer together, the two reflections are mixed, and the radar would “see” only a single object.

Range resolution for a simple pulse is one-half the pulse

length. For two objects to be distinguished, they must be separated in range by at least half the pulse length. The slant range merely refers to the line between the object and the antenna.

$$\text{Range resolution for a simple pulse} = \frac{cT}{2}$$

Range resolution for such a pulse is completely dependent on the pulse duration, and even for a pulse of very short duration, perhaps one-millionth of a second, the pulse length is significant. Such a pulse would yield a slant range resolution of 150 m. It is possible to shorten the pulse, but this requires substantial power and it is simply not feasible to provide good range resolution with simple pulses.

Fortunately, a so-called chirped pulse can be used to solve this problem. A chirped pulse is one in which the frequency varies within the pulse. Figure 22 compares a simple pulse of fixed frequency with a chirped pulse in which the frequency is varied in a steady, or linear, rate. The term “chirp” is used because a sound wave of this form sounds like a bird’s chirp.

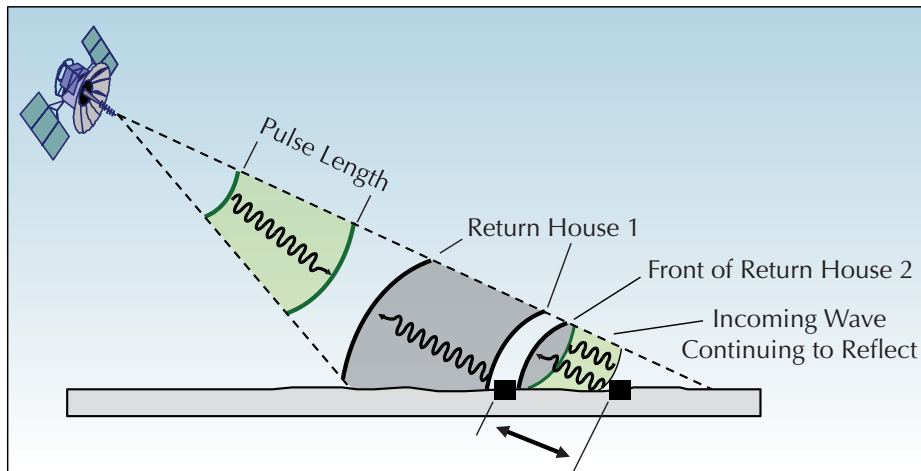


Figure 20. Two distinct reflections. To distinguish two ground features in the slant range direction, the reflected signals must be received separately by the antenna.

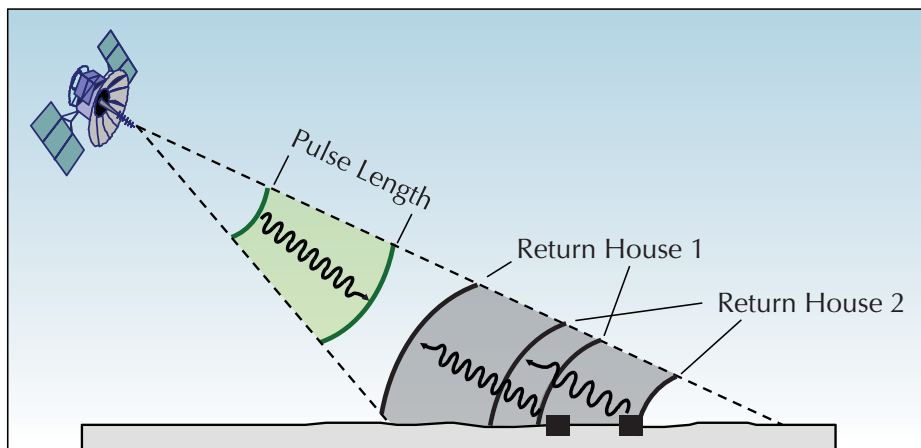


Figure 21. Mixed reflections. In this case the two houses are closer and the reflections are mixed together. Only one feature will be seen on the image.

The relationship between the time duration of a pulse and its bandwidth (B) is $T = 1/B$. Substituting this value into the equation for range resolution yields

$$\text{Range resolution} = \frac{c}{2B}.$$

The essential issue is that for chirped pulses, B is the frequency variation within the pulse. Thus, chirped pulses do not require unreasonably short time durations to yield large bandwidths and improved range resolution. The effective time duration of a chirped pulse is the inverse of its frequency variation. This yields a powerful statement:

$$\text{Range resolution for a chirped pulse} = \frac{c}{2 * \text{Pulse frequency variation}}.$$

This is another remarkable radar resolution equation. Range resolution depends solely on the frequency variation of the pulse, and it has nothing to do with distance or duration of the pulse. Again, commercial space radars provide a good example of the operational implementation of radar imaging principles. These systems currently have a maximum pulse bandwidth of 300 to 400 MHz, which results in a range resolution of approximately 0.5 m. It is interesting to note that some commercial companies are considering substantial increases to the transmitted bandwidth for their next generation systems.

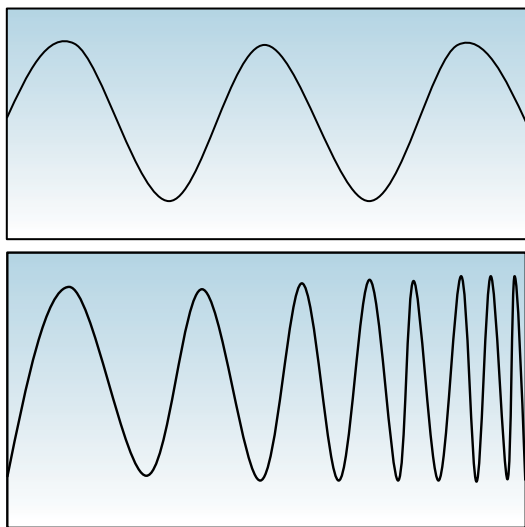


Figure 22. Simple pulse vs. chirped pulse.

Ground Range Resolution

The previous discussion applies to resolution in the slant range direction. The final radar image is projected to a ground surface, and when this is done, the pixel dimensions in range are elongated. Notice in Figure 23 that the slant range resolution component is projected to the ground as a function of the grazing angle. Ground resolution actually degrades for steeper collections. This is opposite the effect for optical images, where the best resolution is at nadir. The reader can imagine that a very shallow grazing angle would yield slant- and ground-range resolutions that are roughly equivalent, and an extremely steep collection angle would yield substantially elongated ground-range resolution cells. For the mid-range collection angles of commercial space radars, the 0.5 m maximum for slant range resolution converts to approximately 1.0 m on the ground.

A Final Observation Regarding SAR Resolution

Of course, distance does matter in radar imaging. Long ranges result in very weak backscatter signals, and building space radar systems requires powerful and sensitive antennas. However, the SAR technique, used in combination with chirped pulses, results in azimuth and range resolutions that are both independent of the distance between the sensor and the ground. This is simply not possible for passive remote-sensing systems that record reflected sunlight or emitted thermal radiation. We began our discussion with expressions for the azimuth and range resolutions of simple radars that were severely limited and replaced them with expressions that are elegant and powerful.

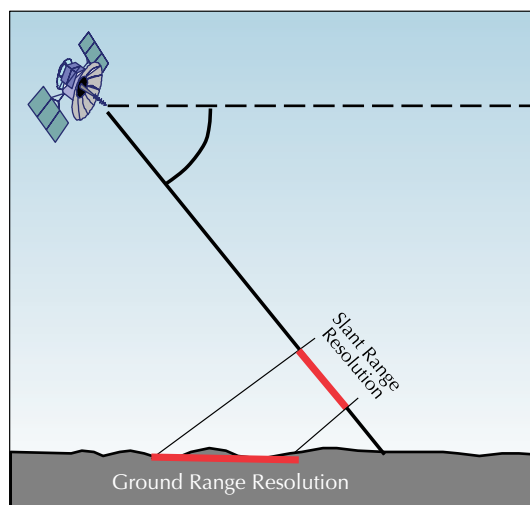


Figure 23. Ground range resolution.

SAR PRODUCT FORMATION

It is important to keep in mind that a radar imaging system does not really know anything of imagery. The radar has no lens to focus light energy onto digital detectors from which image pixels are derived. A SAR knows only about its raw measurements of time, amplitude, and phase, and they are manipulated with signal processing algorithms into images and other products.

Figure 24 shows a simple diagram of the processing flow for SAR products. The raw radar measurements are processed into phase history data, which contains the echo measurements and timing data needed for further processing. A phase history data file is not an image product and cannot be viewed, but it is processed into a pixel form called a “complex image.” Notice that the complex image is a core radar product used to create amplitude images and many other radar products that cannot be generated from simple amplitude data alone. (Note that some of the derived products, such as subsidence maps and elevation models, require more than one complex image.)

A complex image is different than a conventional image in that a traditional image has one value, brightness, for each pixel, while a radar complex image has two values for each pixel. These values can be thought of as amplitude and phase. The amplitude data contain the traditional brightness information for each pixel, and the phase data contain the very precise relative timing information needed for advanced processing.

The complex image displayed in Figure 25 is from the COSMO-SkyMed commercial SAR. The image on the top displays the amplitude data. The image on the bottom was created from the same collection operation, but it displays the associated phase measurements for each pixel. The amplitude image is easy to interpret while the associated phase image appears to include only a random scattering of measurements. This is misleading because phase measurements are precise and of great value.

The technique called persistent scatterer interferometry demonstrates the value of phase information. Multiple radar collections of a site are taken over time from nearly the same location in space, and the resultant phase images are processed to measure very subtle ground surface changes. The microwave illumination is consistent from image to image, and this stands in contrast to sunlight illumination, which is not coherent and which varies considerably due to weather differences. If the radar imaging is controlled so that the ground is illuminated multiple times by the same sensor, from locations that vary by only a short baseline distance, then the phase signatures of stable ground objects can be compared to calculate changes in distances between the scatterers and the antenna.

Phase measurements are so sensitive that inconsistent changes like leaf motion cause phase changes. When multi-image phase data are compared, vegetated areas that changed

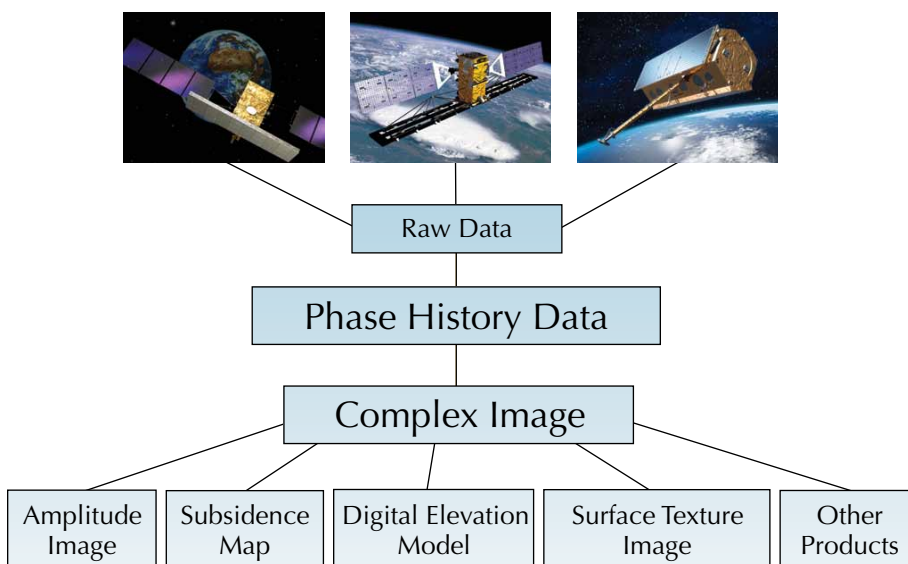


Figure 24. The SAR product formation chain. Example satellite data inputs at top: (left) COSMO-SkyMed. Credit: Telespazio; (center) RADARSAT-2. Credit: MD Robotics Ltd.; (right) TerraSAR-X. Credit: EADS Astrium

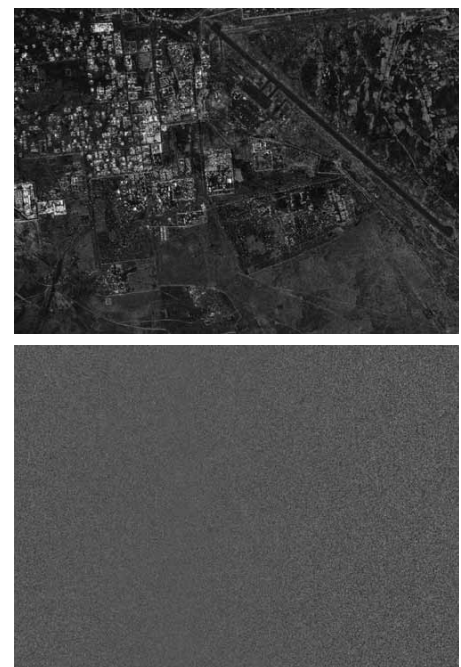


Figure 25. The SAR complex image, COSMO-SkyMed. © e-GEOS. All Rights Reserved

due to wind and rain are often “de-correlated”; their phase signatures cannot be matched from image to image. However, the phase signatures of stable ground objects can be used to determine very subtle changes in surface structure over time. The example in Figure 26 shows surface subsidence around an oilfield in Kuwait. This subsidence map was generated from a stack of 16 TerraSAR-X images collected between 2008 and 2011. The map shows ground deflation due to oil field depletion. The subsidence is occurring at the rate of about 10 mm per year in the red areas. This is remarkable sensitivity, especially considering that the measurements were made by a spacecraft more than 800 km distant.

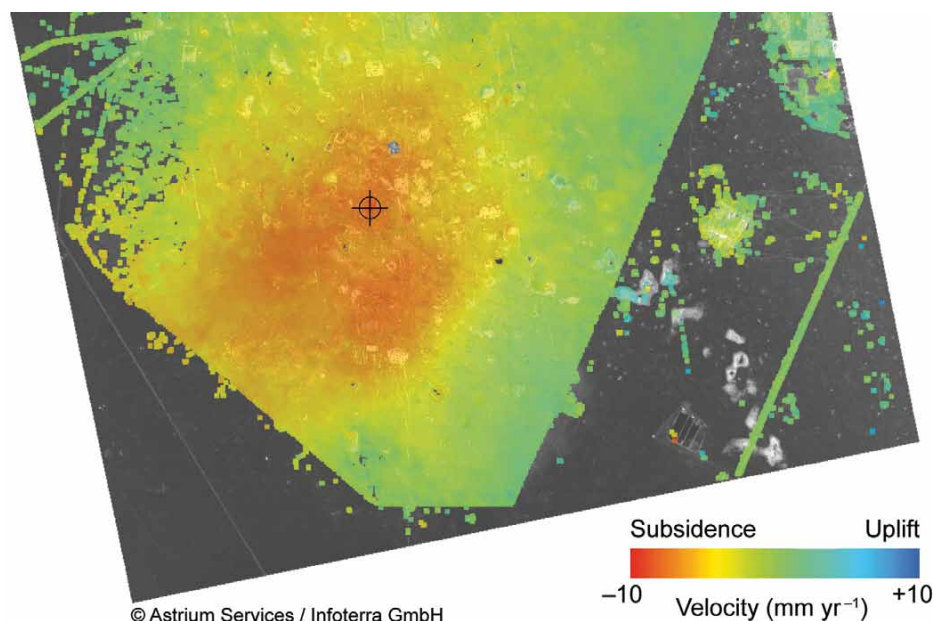


Figure 26. Surface subsidence map, TerraSAR-X Collections.
© Astrium Services / Infoterra GmbH

SPACE-BASED SAR SYSTEMS

Space-based SAR is particularly suited to ocean applications because satellites have global access and offer repeated collection opportunities to observe the changing state of marine phenomena. A number of space systems have been launched since Seasat first demonstrated the value of space SAR in 1978. These systems include the NASA space shuttle instruments called Spaceborne Imaging Radar (SIR) A, B, and C that operated in the 1980s and early 1990s. The SIR-C system was innovative in that it included X-, C-, and L-band sensors on a single large antenna, and it also supported quad-polarization. The Soviet Union launched ALMAZ (S-band) in 1991, and in the same year the Europeans launched ERS-1 (C-band). In 1992, Japan launched JERS-1, which was L-band like Seasat and the early SIR missions. These were followed by additional European and Japanese systems and, in 2000, a NASA mission called Shuttle Radar Topography Mission (SRTM) that included two antennas separated by a 60 m mast and used interferometry to generate a near-global elevation model.

More recently, high-resolution SARs were launched by Canada (RADARSAT-2, C-band), Italy (COSMO-SkyMed, X-band), and Germany (TerraSAR-X and TanDEM-X, X-band). These SARs have resolutions as good as 1 m. They also include wide-swath ScanSAR modes that can cover areas hundreds of kilometers wide. COSMO-SkyMed, which is a constellation of four satellites, and TerraSAR-X, are both dual-pol systems, and RADARSAT-2 is quad-pol. The Germans have also launched a twin satellite called TanDEM-X, which flies in formation with TerraSAR-X, to support an interferometric mission, similar to SRTM. However, the TerraSAR-X/TanDEM-X pair will collect data for about three years, not just 11 days as did SRTM, and their data will be used to generate elevation information for the entire globe at a rate that is appreciably more dense than the best SRTM data. These systems illustrate the emergence of high-resolution, very capable spaceborne SAR systems to support commercial and government applications on a global scale.

AN OVERVIEW OF OCEAN APPLICATIONS OF SAR IMAGING

For ocean applications, it is important to keep in mind that radar energy cannot penetrate water by more than a few millimeters. A SAR's interaction with the surface depends on the radar wavelength and polarization, incidence angle, and surface roughness. SAR backscatter results from the radar's interaction with small, wind-induced waves, called Bragg waves, that are similar in size to the radar wavelength. SAR detects these Bragg waves, and thus can observe currents and eddies on the ocean surface. Figure 27 illustrates SAR's sensitive detection of water surface structure, showing waves, ships, and ship wakes in the Strait of Gibraltar. Cross-polarized images (HV or VH) can sometimes be used to suppress ocean signatures and better highlight ship signatures.

Objects that are moving along the line-of-sight of the radar are displaced from their actual locations. This is evident in Figure 27 where ship signatures are displaced from their wakes. The magnitude of the displacement can be used to estimate ship speed. In this image, one can clearly see all ship traffic and the direction of ship motion, and, in some cases, speed can be estimated.

It is easy to imagine the value of combining SAR ship-detection images with coincident Automated Identification System (AIS) data used to characterize a ship's identity, position, and course. In this way, ships that are not emitting AIS information can be identified in the SAR image for tracking and, perhaps, physical searching. The follow-on mission to RADARSAT, called the RADARSAT Constellation Mission, will include three satellites that carry AIS receivers to collect information over the area covered by the SAR images.

Oil and surfactants tend to suppress Bragg waves and are usually darker on radar images than surrounding water (see

Caruso et al., 2013, in this issue). Oil from the Deepwater Horizon spill is quite evident in the RADARSAT image shown in Figure 28. Radar can penetrate ice on the order of a few wavelengths, and this creates volume scattering, which provides a brighter signature for ice than surrounding water, as seen in Figure 29 (see discussions in Jackson and Apel, 2004, and Dierking, 2013, in this issue).

The small surface waves that SAR is so good at detecting can also be used to extract other information not directly apparent on the image itself. For example, it is possible to calculate wind speed and direction (Gierach et al., 2012) and to detect activities and structures below the ocean surface, such as underwater currents and shoals. Radar has also been used to measure current speed in rivers via a technique called along-track interferometry, which uses phase data collected by two antennas separated along the line of flight. An experimental mode of TerraSAR-X provides two phase centers with a 0.8 m baseline, and this has shown promise for deriving current speeds to within 0.1 m s^{-1} (Romeiser et al., 2007, 2010; Romeiser and Runge, 2007; Romeiser, 2013, in this issue).

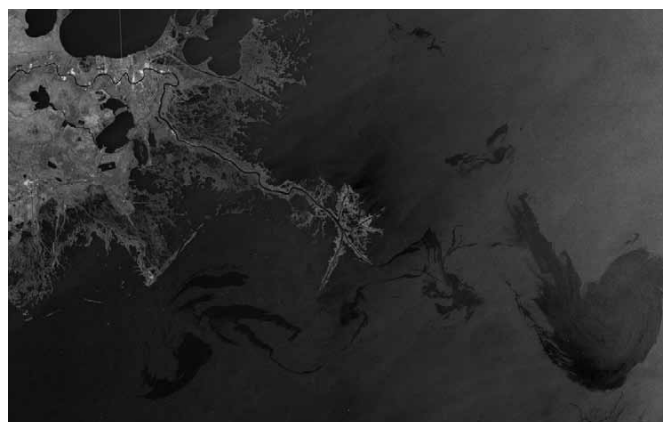


Figure 28. Gulf oil spill, RADARSAT-1. © MacDonald, Dettwiler and Associates Ltd. All Rights Reserved



Figure 27. Ship and wake detection, Strait of Gibraltar, TerraSAR-X. © Astrium Services / Infoterra GmbH

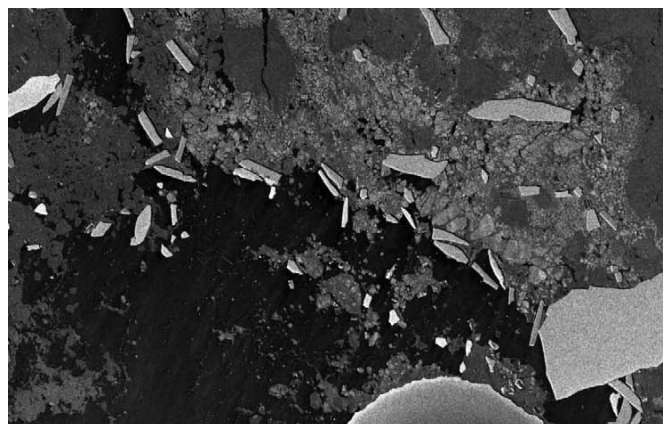



Figure 29. Arctic ice, COSMO-SkyMed. © e-GEOS. All Rights Reserved

SUMMARY OF SAR IMAGING

Earth is an ocean planet that is always partially covered in clouds and haze. Radar is the only remote-sensing technology that enables imaging under such conditions, and this is its primary benefit. However, radar's inherent precision and natural coherence, along with the techniques of aperture synthesis and chirped pulses have combined over the past several years to revolutionize the value of radar imaging. There are now three commercial space radar programs that can routinely collect images with 1 m resolution, regardless of the range to the ground, and that can also vary their coverage and resolution to image large ground areas and wide open-ocean regions. There are also airborne radars that provide long swaths of image mosaics and accurate elevation models.

Such systems have numerous applications beyond guaranteed collection regardless of cloud cover. The list includes oil spill and open-ocean ship detection; Arctic ice, flood, coastal, topographic, riverine, and deforestation mapping; precise measurements of ground motion caused by surface subsidence, earthquakes, landslides, and volcanic activity; glacial advance and retreat monitoring; port and harbor monitoring; facility monitoring; and many others.

Synthetic aperture radar was a tremendous advance in image processing that enabled high-resolution imaging from any distance, giving SAR a unique ability among all imaging technologies. SAR imaging is now being combined with other commodity technologies, such as differential GPS and fast and inexpensive computer processing. Together, these technologies are revolutionizing radar processing by enabling product generation capabilities that were unattainable just a few years ago.

Perhaps the best example of the implementation of precision SAR imaging is the German TanDEM-X mission, which is creating a contiguous high-resolution elevation model over the entire planet (German Aerospace Center, Microwaves and Radar Institute, 2013). There are twin radar spacecraft flying in formation, within 200 m of each other, while emitting and recording pulses of microwave radiation. All of the measurements of orbital motion, range, amplitude, and phase are being carried out with the highest precision, independent of clouds and distance, because that is the nature of SAR imaging. 

REFERENCES

- Ager, T.P. 2001. Active sensing systems. Pp. 301–349 in *Modern Photogrammetry*. E.M. Mikhail, J.S. Bethel, and J.C. McGlone, eds, John Wiley & Sons.
- Carrara, W.G., R. M. Majewski, and R.S. Goodman. 1995. *Spotlight Synthetic Aperture Radar: Signal Processing Algorithms*. Artech House, 554 pp.
- Caruso, M.J., M. Migliaccio, J.T. Hargrove, O. Garcia-Pineda, and H.C. Graber. 2013. Oil spills and slicks imaged by synthetic aperture radar. *Oceanography* 26(2):112–123, <http://dx.doi.org/10.5670/oceanog.2013.34>.
- Curlander, J.C., and R.N. McDonough, 1991. *Synthetic Aperture Radar: Systems and Signal Processing*. John Wiley & Sons, 647 pp.
- Dierking, W. 2013. Sea ice monitoring by synthetic aperture radar. *Oceanography* 26(2):100–111, <http://dx.doi.org/10.5670/oceanog.2013.33>.
- German Aerospace Center. 2010. *TerraSAR-X Ground Segment Basic Product Specification*, Issue 1.7. 109 pp., <http://www.astrium-geo.com/na/1249-terrasar-x-technical-documents>.
- German Aerospace Center, Microwaves and Radar Institute. 2013. *TanDEM-X Science Home*, <http://www.dlr.de/hr/en/desktopdefault.aspx/tabid-2317>.
- Gierach, M.M., H.C. Graber, and M.J. Caruso. 2012. SAR-derived gap jet characteristics in the lee of the Philippine Archipelago. *Remote Sensing of Environment* 117:289–300, <http://dx.doi.org/10.1016/j.rse.2011.10.004>.
- Italian Space Agency. 2009. *COSMO-SkyMed SAR Products Handbook*, rev. 2. 105 pp., <http://www.e-geos.it/products/pdf/csk-product-handbook.pdf>.
- Jackson, C.R., and J.R. Apel, eds. 2004. *Synthetic Aperture Radar Marine User's Manual*. US Dept of Commerce, 464 pp.
- Jakowatz, C.V., D.E. Wahl, P.H. Eichel, D.C. Ghiglia, and P.A. Thompson. 1996. *Spotlight-Mode Synthetic Aperture Radar: A Signal Processing Approach*. Springer Science, 448 pp.
- MacDonald, Dettwiler and Associates Ltd. 2009. *RADARSAT-2 Product Description*, Issue 1/6, 46 pp., http://gs.mdacorporation.com/products/sensor/radarsat2/RS2_Product_Description.
- Oliver, C., and S. Quegan. 2004. *Understanding Synthetic Aperture Radar Images*. SciTech Publishing, 464 pp.
- Romeiser, R. 2013. The future of SAR-Based oceanography: High-resolution current measurements by along-track interferometry. *Oceanography* 26(2):92–99, <http://dx.doi.org/10.5670/oceanog.2013.37>.
- Romeiser, R., and H. Runge. 2007. Theoretical evaluation of several possible along-track InSAR modes of TerraSAR-X for ocean current measurements. *IEEE Transactions on Geoscience and Remote Sensing* 45:21–35, <http://dx.doi.org/10.1109/TGRS.2006.885405>.
- Romeiser, R., H. Runge, S. Suchandt, J. Sprenger, H. Weilbeer, A. Sohrmann, and D. Stammer. 2007. Current measurements in rivers by spaceborne along-track InSAR. *IEEE Transactions on Geoscience and Remote Sensing* 45:4,019–4,030, <http://dx.doi.org/10.1109/TGRS.2007.904837>.
- Romeiser, R., S. Suchandt, H. Runge, U. Steinbrecher, and S. Grünler. First analysis of TerraSAR-X along-track InSAR-derived current fields. *IEEE Transactions on Geoscience and Remote Sensing* 48:820–829, <http://dx.doi.org/10.1109/TGRS.2009.2030885>.
- Stimson, G.W. 1998. *Introduction to Airborne Radar*. Scitech Publishing, 576 pp.
- Ulaby, F.T., R.K. Moore, A.K. Fung. 1986a. *Microwave Remote Sensing: Active and Passive*, vol. 1: *Fundamentals and Radiometry*. Artech House, 456 pp.
- Ulaby, F.T., R.K. Moore, A.K. Fung. 1986b. *Microwave Remote Sensing*, vol. 2: *Radar Remote Sensing and Surface Scattering and Emission Theory*. Artech House, 608 pp.
- Ulaby, F.T., R.K. Moore, A.K. Fung. 1986c. *Microwave Remote Sensing*, vol. 3: *From Theory to Applications*. Artech House, 1,120 pp.
- Van Zyl, J.J., and K. Yunjin. 2011. *Synthetic Aperture Radar Polarimetry*. John Wiley & Sons, 647 pp.